

# Optimizing the parameterization of mass flow models

J. Krenn

*University of Natural Resources and Life Sciences (BOKU), Vienna, Austria*

M. Mergili

*University of Natural Resources and Life Sciences (BOKU), Vienna, Austria*  
*University of Vienna, Vienna, Austria*

J.T. Fischer

*Department of Natural Hazards, Austrian Research Centre for Forests (BFW), Innsbruck, Austria*

P. Frattini

*University of Milano-Bicocca, Milan, Italy*

S.P. Pudasaini

*University of Bonn, Bonn, Germany*

**ABSTRACT:** The parameter set up of mass flow models decides on the quality of the results. We present a novel parameter optimization procedure, building on the comparison of model results and observed deposition areas. As it is evident that natural conditions cannot be represented by one constant value for larger areas we suggest using input value ranges rather than discrete values. The proposed procedure consists in a stepwise optimization of the input parameter values and ranges by using the precedent results as input for the next step. The procedure is applicable to any type of single-value input parameter and any type of mass flow propagation model. We use two GIS-based open source modelling tools: (i) the conceptual r.randomwalk and (ii) the complex physically-based r.avaflow. Both tools are capable to process value ranges of input parameters. The still ongoing study aims to derive reliable guiding values for various process types to be used for forward calculations. We demonstrate the procedure using two rock avalanche events (Acheron and Black Rapids). The first outcomes are promising, but more work is necessary to confirm and extend the validity of the results.

## 1 INTRODUCTION

The choice of input parameters is crucial to obtain satisfactory results for any type of model dealing with mass flows such as rock avalanches, debris flows, or snow avalanches—be it a complex physically based or a simpler conceptual one. Unfortunately, parameter values are often uncertain due to lacking information of the pre-failure conditions, inaccessible terrain, high spatial variability or other factors. Therefore, parameters have to be optimized through the back-calculation of well-documented events before they can be applied to forward calculations.

Parameter optimization or sensitivity analysis efforts often consist in varying the value of one parameter while keeping the others fixed (one-at-a-time method). However, Saltelli et al. (2010) consider this approach inappropriate as it does not account for the complexity of the issue. Instead, multiple parameters would have to be considered at once.

Further, it is common practice to work with discrete values as input parameters. In this sense, the tool AIMEC (Fischer 2013) facilitates the optimization and sensitivity analysis procedure for multiple input values and also supports evaluation and comparison of complex model outputs. However, natural conditions—which every mass flow model tries to simulate—are variable in space and time and cannot accurately be described by one single value for a larger area.

In the present work we suggest, demonstrate and discuss a novel procedure to optimize the parameterization of mass flow models (i) including multiple parameters at once, and (ii) considering parameter ranges in addition to single values. (iii) We show how to use this procedure to find guiding parameter values for specific types of mass flow processes, exemplified with rock avalanches. It shall be emphasized that we only consider the propagation of mass flows, based on given release areas.

We demonstrate the newly developed procedure for two contrasting open source GIS-based model applications accepting parameter value ranges as input: the conceptual tool *r.randomwalk* (Mergili et al. 2015b) and the complex physically-based dynamic model *r.avaflow* (Mergili et al. 2015a).

## 2 STUDY AREAS

### 2.1 Acheron Rock Avalanche, New Zealand

The Acheron Rock Avalanche in Canterbury, New Zealand, occurred approx. 1,100 years BP (Smith et al., 2006). Mergili et al. (2015b) estimated a release volume of 6.4 million m<sup>3</sup> from a topographic reconstruction. We use a 10 m resolution DEM derived by stereo-matching of aerial photographs. Impact, release and deposition areas are derived from field and imagery interpretation as well as from data published by Smith et al. (2006). The impact area of this event is subject to a sharp turn in its upper section, which is a consequence of the deflection by the steep counter slope. The moving mass produced a significant run-up in some areas and then followed the main valley.

### 2.2 Black Rapids Rock Avalanche, Alaska (Eastern event)

The Black Rapids Rock Avalanches were triggered by the M7.9 Denali fault earthquake of 3 November 2002. Among other mass flows, the earthquake triggered 3 large rock avalanches propagating onto the Black Rapids Glacier (Jibson et al. 2006). In the present study the largest eastern event is employed for the parameter optimization procedure. The volume of the rock avalanche was estimated at 13.9 million m<sup>3</sup> by Jibson et al. (2006). A digital elevation model based on IFSAR (Interferometric Synthetic Aperture Radar) data for Alaska is used (data available from the U.S. Geological Survey).

During the event the debris ran up a 50 m high lateral moraine (Sosio et al. 2012) leaving it covered by a sheet of rock avalanche material. The deposit on the Black Rapids Glacier is clearly constrained. Shortly after the event the deposit thickness was estimated at 2–3 m on average (Jibson et al. 2006). Until today the debris sheets significantly reduce the ablation during summer months (Shugar and Clague, 2011). As a result the covered area almost conserves its height while the uncovered area is subject to ablation. This effect has led to a height difference of more than ten meters yet.

## 3 METHODOLOGY

We suggest a procedure for optimizing the parameterization of mass flow modelling approaches. The main focus of this work consists in investigating their capacity to reproduce the deposition area of observed events. This capacity is quantified by the area under the ROC (receiver operating characteristic) Curve— $AUC_{ROC}$ , a value in the range 0–1. While 1 stands for an exact overlap of the simulated and observed deposition areas, 0.5 represents a random distribution of pixels (model failure; see Fig. 1). In this context we (i) use the Acheron and Black Rapids Rock Avalanches to demonstrate how to find guiding ranges of parameters. They should be applicable for specific process types after analysing multiple, comparable events. (ii) We compare the quality of the results of *r.randomwalk* and *r.avaflow*, using the example of the Acheron Rock Avalanche.

We focus on testing ranges with both simulation tools; nevertheless also single values are tested to compare the general quality of the results.

It shall be emphasized that the current work mainly represents an introduction to the procedure, employing two examples in order to demonstrate the delineation of the guiding values. However, to obtain reliable values more observed events as well as forward calculation tests are necessary. All this will be done in the framework of an ongoing project.

### 3.1 The tools *r.randomwalk* and *r.avaflow*

Firstly, *r.randomwalk* is used to represent the branch of conceptual approaches. The tool is based on a constrained random walk method which allows to route mass points through a digital elevation model until one or more defined break criteria are fulfilled (Mergili et al. 2015b). In the present work, the break criteria build on the angle of reach and on the two-parameter friction model of Perla et al. (1980). *r.randomwalk* can be used for single events, but is also particularly suitable to derive potential impact areas at broader scales.

Secondly, *r.avaflow* (Mergili et al. 2015a), building on the Pudasaini (2012) two-phase flow model, is applied to analyze the general functionality of

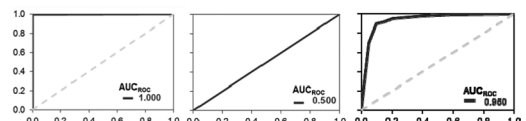


Figure 1. Examples of ROC plots with  $AUC_{ROC} = 1$  (best possible result),  $AUC_{ROC} = 0.5$  (model failure),  $AUC_{ROC} = 0.95$  (realistic result of a good simulation).

the optimization method for more complex physically-based dynamic simulation tools. This tool is particularly suitable for detailed analyses of single events, yielding values for phase velocities, phase heights, pressures, energies etc.

Both simulation tools are implemented as modules of the software GRASS GIS (GRASS Development Team, 2015). They support the execution of multiple model runs in parallel, each model run building on a set of randomized input parameters. The randomization of the parameter values is constrained by a user-defined range (minimum and maximum) of each parameter. The results of all simulation runs are collected into an impact indicator index III map, denoting the fraction of model runs predicting an impact on a given pixel. III is evaluated against the observed deposition area by means of an ROC plot (see Fig. 1).

### 3.2 Parameter optimization procedure for r.randomwalk

Two functionalities of the tool are tested. (i) The set of general random walk parameters (see Table 1) governing lateral spreading and the smoothness of the flow path are optimized, while keeping the break criterion constant at the observed angle of reach. (ii) The two-parameter friction model introduced by Perla (1980) is applied, where the physical parameters  $\mu$  and M/D are optimized.

Generally speaking, the testing procedure is based on an iterative process. The parameter values proposed by Mergili et al. (2015b) are used to perform a first set of model runs. Single values on the one hand (e.g.  $L_{ctrl} = 400$  m) and value ranges (e.g.  $L_{ctrl} = 400 - 800$  m) on the other hand are applied to test the general parameters of r.randomwalk (see Table 1). Thereby 100 randomized parameter combinations are chosen for each parameter range or combination of ranges.

After a first series of sets of model runs using the suggested values for  $L_{seg}$ ,  $R_{max}$ ,  $f_\beta$  and  $f_d$  and varying the range or value of the first parameter ( $L_{ctrl}$ ), the results are investigated. Thereby the input value of  $L_{ctrl}$  that produced the best  $AUC_{ROC}$  (i.e. closest to 1.0; see Mergili et al. 2015b for a closer description of an ROC curve) is selected as input value range or single value in the next model run. The procedure is repeated i.e. the number of already optimized parameter values or ranges increases until an optimized value for all parameters is obtained (see Fig. 2a, 1st Cycle). Next, a second cycle of simulations is performed using the best values of the first cycle as starting values and performing the variation procedure again for each parameter (see Fig. 2b, 2nd Cycle). In principle, additional cycles have to be performed until the  $AUC_{ROC}$  values remain constant.

Table 1. General parameters included in the optimization process for r.randomwalk (see Mergili et al. 2015b for details).

Parameter	Name	Starting value	Tested interval*
$L_{ctrl}$	Control Length	1000 m	400–2500 m
$L_{seg}$	Segment length	100 m	30–700 m
$R_{max}$	Maximum run-up	10 m	5–50 m
$f_\beta$	Slope factor	5	1–20
$f_d$	Direction factor	2	0.5–10

\* "Tested interval" refers to the entire investigated range, various sub-ranges and values are tested within this interval.

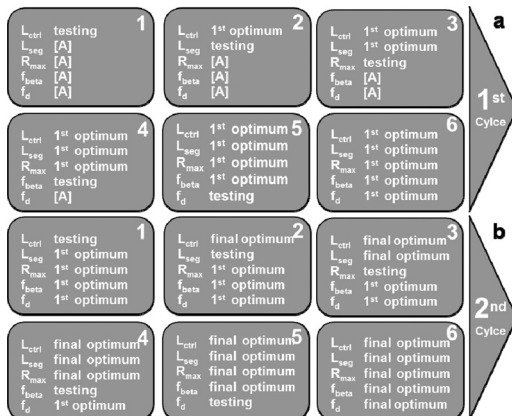


Figure 2. Optimization procedure for the general parameters of r.randomwalk; [A] estimated starting value (see Table 1).

R.randomwalk includes the 2-parameter friction model introduced by Perla et al. (1980). The motion of the mass flow is influenced by  $\mu$ , which represents the sliding friction coefficient and by M/D, a mass-to-drag ratio. While M/D has more influence on velocity in steep track sections,  $\mu$  governs the velocity in the run-out area (Wichmann et al. 2003). The flow velocity  $v$  is updated during each step of the routing procedure, and the flow stops as soon as  $v \leq 0$ . This model was originally developed for snow avalanches, but has also been applied to debris flows (Zimmermann et al. 1997, Mergili et al. 2012) and to rock avalanches.

The same type of procedure as applied to the general random walk parameters (see Table 1) before is also used to optimize  $\mu$  and M/D (see Fig. 3). Due

to the presence of only two parameters, the optimization procedure is shorter for this application. At the beginning certain ranges of  $\mu$  are tested for a number of fixed values of M/D. This step is necessary as—in contrast to the general parameters—no reliable estimate of this parameter was available in advance. A plausible interval for the input parameters was derived from published data of Perla et al. (1980), Gamma (2000), Vilajosana et al. (2007), Jónasson et al. (1999), Baumann (2011) and Wichmann et al. (2003). These intervals will be subject to investigation and are listed in Table 2. While the values were previously applied to snow avalanches and debris flows only, we explore whether they produce reasonable results for rock avalanches too.

In the next step the optimized range of  $\mu$  (best  $AUC_{ROC}$  result) is applied to test various ranges of M/D. After this has been performed, the first cycle is finished and a second one is initiated. Here the optimized range of M/D is kept constant during a set of model runs while varying  $\mu$  with the same ranges as before. It is investigated whether

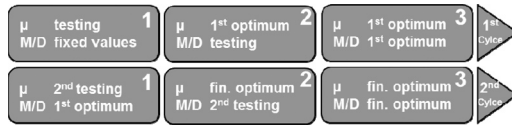


Figure 3. Optimization procedure for  $\mu$  and M/D as input values of the 2-parameter friction model of Perla et al. 1980; functionality test for rock avalanches using r.randomwalk.

Table 2. Parameters included in the optimization process for the 2-parameter friction model.

Parameter	Name	Tested interval
$\mu$	Friction coefficient	0.02–0.54
M/D	Mass-to-drag ratio	100–15000

Table 3. Parameters included in the optimization process for r.avafow (see Pudasaini 2014 & Pudasaini et al. 2014 for details).

Para-meter	Name	Starting value	Tested interval*
$U_T$	Terminal velocity	1 m/s	0.1–10
$\delta$	Bed friction angle	20 °	5–40
$\phi$	Internal friction angle	35 °	20–45
$C_{VM}$	Virtual mass	0.5	0.1–500
$Re_p$	Particle Reynolds number	1	1–100
$\chi$	Viscous shearing coefficient	0	0–3
$N_R$	Quasi Reynolds number	30000	$10^3$ – $10^8$
$N_{RA}$	Mobility number	1000	$10^2$ – $5 \times 10^5$

\* “Tested interval” refers to the entire investigated range, various sub-ranges and values are tested within this interval.

the  $AUC_{ROC}$  results increase again or the range that produces the best  $AUC_{ROC}$  result changes. In the last step the 2nd optimized range of  $\mu$  is in turn applied to vary the values of M/D a second time and to obtain the final parameter optimum for M/D.

### 3.3 Parameter optimization for r.avafow

r.avafow represents a more complex simulation approach with a physically based flow model and requires several input parameters. The procedure is demonstrated for eight selected input parameters of r.avafow. The tested parameter ranges are derived from the physical basis in Pudasaini (2014), from empirical values for rock avalanches, and from expert knowledge (see Table 3). The optimization follows the same type of iterative procedure described for r.randomwalk (see Fig. 4). However, only one optimization cycle is performed. 48 randomized parameter combinations are tested for each range or combination of ranges.

r.avafow is capable to produce various types of results, however, for the current work only the impact area is of main interest for the computation of the impact indicator index.

### 3.4 Visualization and derivation of guiding values as a basis for future modelling campaigns

In order to obtain guiding parameter sets as a basis for forward simulation of rock avalanches—or other types of mass flow processes—it is necessary to find an overlapping value range for each parameter in the results of all tested events. For this purpose the  $AUC_{ROC}$  values for each parameter value or range are visualized and examined in a plot of the type displayed in Fig. 5. The plot indicates that the highest  $AUC_{ROC}$  values of both events (representing value ranges in this case) overlap in an interval from 800–1000 meters of the arbitrary sample parameter. The general idea

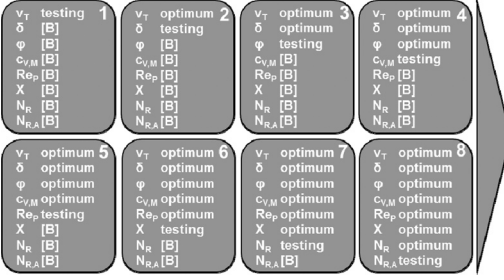


Figure 4. Optimization procedure r.avafow; [B] = estimated starting value (see Table 3).

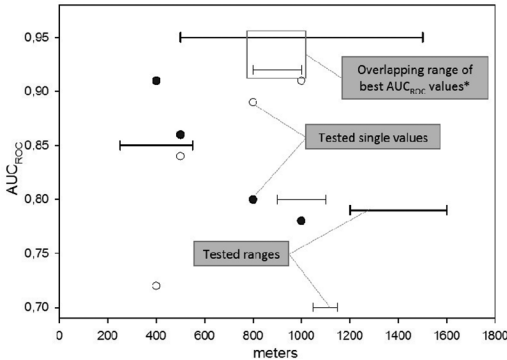


Figure 5. Sample Plot, derivation of overlapping value ranges; each event is displayed in a particular shade of grey, enabling the comparison of the  $AUC_{ROC}$  levels associated to different events.

is to utilize the value range as the desired guiding range for future forward modelling campaigns. In case there is no clear overlap of the best  $AUC_{ROC}$  results, the best possible values or ranges that show an overlap are used.

Considering that it is certainly necessary to back-calculate more than two events to obtain valid estimates for a given process type, Fig. 5 suggests a procedure to visualize findings also for a large number of events.

## 4 PRELIMINARY RESULTS

### 4.1 r.randomwalk—general parameters

After performing the optimization procedure described in Section 3.2, the resulting  $AUC_{ROC}$  values are evaluated and compared among each other. Even though the proposed procedure does not represent a sensitivity analysis as such, the contribution of each parameter to the overall result is quantified by the increase in the  $AUC_{ROC}$  value after each step. In detail the resulting  $AUC_{ROC}$  val-

ues for the Acheron Rock Avalanche feature an increase from 0.846 after a first simulation using the estimated values stated by Mergili et al. (2015b) to 0.959 after the first optimization cycle (see Figure 6). The second cycle does not show a significant enhancement concerning the quality of the results. Instead, the  $AUC_{ROC}$  values maintain the same level with a slight increase at the beginning and a slight decrease after the last optimization steps. These deviations are likely to reflect the not yet quantified random component in the results.

The same procedure is performed for the Black Rapids Rock Avalanche. The results (see Fig. 7) show similar characteristics as observed for the Acheron Rock Avalanche. They start with an  $AUC_{ROC}$  value of 0.843 and increase to 0.980 after the first cycle. Again the second cycle only shows slight changes and finally reaches a value of 0.986. Focusing only on  $AUC_{ROC}$  values, the second cycle may be neglected in the procedure, because it does not result in a significant increase of the quality of the result. Nevertheless, the second cycle tends to provide a concretization of some input value ranges and should therefore still be considered.

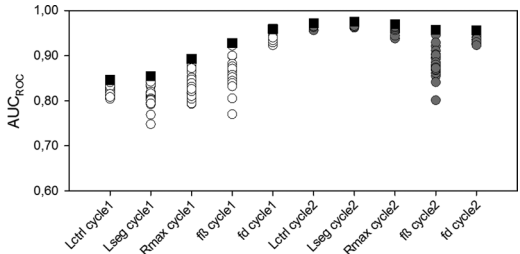


Figure 6. r.randomwalk: Optimization procedure of general random walk parameters for the Acheron Rock Avalanche (markers: white = 1st cycle, grey = 2nd cycle, black = maximum value).

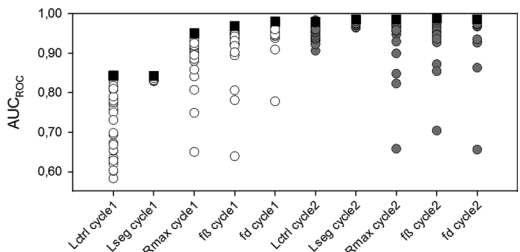


Figure 7. r.randomwalk: Optimization procedure of general random walk parameters for the Black Rapids Rock Avalanche (markers: white = 1st cycle, grey = 2nd cycle, black = maximum value).

Next, the optimized ranges of both events are summarized in resulting plots (see Figure 8) to identify joint intervals which will serve as a guiding value range for forward calculations of comparable processes. The derivation of these guiding ranges is shown for  $L_{ctrl}$  and  $L_{seg}$  in Figure 8. Note that, for reasons of clarity, the scale of the y-axis varies among the plots according to the  $AUC_{ROC}$  value range of the displayed results.

Concerning  $L_{ctrl}$  the optimal overlapping range is identified at 1000–1500 m (see Figure 8a). In this case the overlap does not appear at the best  $AUC_{ROC}$  values of each case study.  $L_{seg}$  features the best possible overlap of 30–80 m at the highest  $AUC_{ROC}$  results of each tested event (see Figure 8b).  $R_{max}$  shows its best overlap at 15–40 m for the highest  $AUC_{ROC}$  value of the Black Rapids Rock Avalanche and the 2nd highest one for the Acheron Rock Avalanche. Finally,  $f_d$  and  $f_\beta$  both feature overlapping ranges for the best values of  $AUC_{ROC}$  obtained for both case studies. While the optimal range for  $f_\beta$  is 1–10, a range of 2–6 is determined for  $f_d$ . Table 4 summarizes the outcomes for all tested parameters.

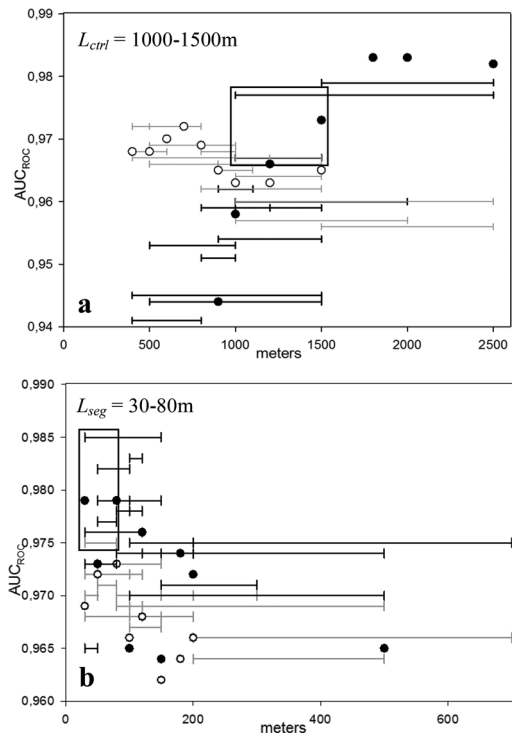


Figure 8. Overlapping ranges of the optimal  $AUC_{ROC}$  values for the general parameters (a)  $L_{ctrl}$  and (b)  $L_{seg}$  of *r.randomwalk* for both tested events.

Table 4. Overview of the optimal value ranges derived for the general parameters of *r.randomwalk*.

Parameter	Optimal range
$L_{ctrl}$	1000–1500 m
$L_{seg}$	30–80 m
$R_{max}$	15–40 m
$f_d$	2–6
$f_\beta$	1–10

We further note that, with a few exceptions, the tested parameter ranges yield higher values of  $AUC_{ROC}$  than the tested single values for each parameter.

#### 4.2 *r.randomwalk*: 2-parameter friction model

The optimization process for  $\mu$  and M/D (2-parameter friction model by Perla et al. 1980) for the Acheron Rock Avalanche shows a satisfying quality at each step of the procedure. However, the  $AUC_{ROC}$  values do not significantly enhance during the process, but vary between 0.962–0.964 (see Figure 9). Both the 1st and 2nd cycle results of  $\mu$  show a distinct gap of values between  $AUC_{ROC} = 0.5$  and 0.85. More closely investigating the results, it is evident that only value ranges including a lower boundary of  $0.02 < \mu < 0.1$  lead to  $AUC_{ROC}$  values  $> 0.85$ . A similar, but smaller data gap occurs for M/D between  $AUC_{ROC} = 0.45 – 0.65$  or a bit lower in the 2nd cycle. In this case the input value ranges between 20–100 lead to a low quality of the results.

A very similar behavior is observed for the Black Rapids Rock Avalanche (see Fig. 10). The highest  $AUC_{ROC}$  values range between 0.976 and 0.978.

The high quality results obtained through the first cycle arise from the selection of the first input M/D value. As there was no estimate available to use as a starting value a series of preliminary tests were performed (see section 3.2) leaving less space for an increase of the quality of the results. A preferable alternative might be to start the procedure from a randomly chosen value within the whole tested interval.

After evaluating the  $AUC_{ROC}$  results also the derived maps of III are of interest. A comparison of the sample plots displayed in Figure 11 shows a significant difference in the simulated deposition areas. A first glance might indicate that the result shown in Figure 11a is of better quality than the result shown in Figure 11b. A closer inspection reveals that “better” results i.e. higher  $AUC_{ROC}$  values are obtained if high values of III cover larger parts of the observed deposition area at the cost of a wider spread of low indices out of the observed boundaries. In terms of practical applicability, this rather conservative result is clearly preferable over

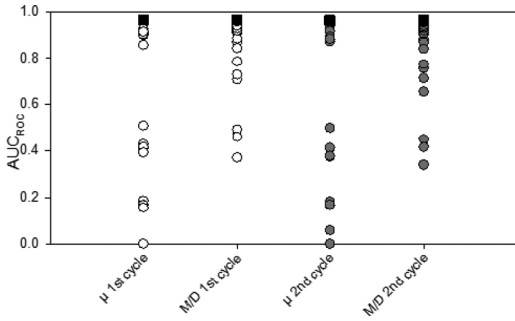


Figure 9. r.randomwalk: Optimization procedure of  $\mu$  and M/D for the Acheron Rock Avalanche (markers: white = 1st cycle, grey = 2nd cycle, black = maximum value).

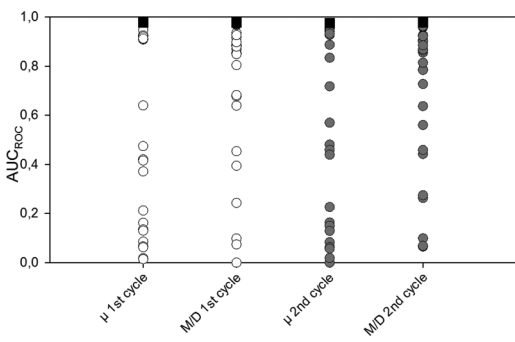


Figure 10. r.randomwalk: Optimization procedure of  $\mu$  and M/D for the Black Rapids Rock Avalanche (markers: white = 1st cycle, grey = 2nd cycle, black = maximum value).

an outcome that displays low values of III for parts of the observed deposition area. However, it shall be emphasized that all pixels with  $III = 0$  outside of the observed impact are excluded from the calculation of  $AUC_{ROC}$ , an approach obviously favouring conservative results. Other—maybe better—strategies for normalizing the area included in the computation of  $AUC_{ROC}$  will be tested in the future.

The guiding values finally derived from the optimization procedure are  $\mu = 0.02 - 0.2$  and  $M/D = 15000$ . In the case of  $M/D$  not a value range but a single value reached best  $AUC_{ROC}$  results. The delineation was performed as displayed in Figure 5. We note that a higher number of tested events will be necessary to derive more robust guiding values.

#### 4.3 r.avaflow

The optimization procedure was applied to the Acheron Rock Avalanche in order to obtain an optimal combination of parameters for this event.

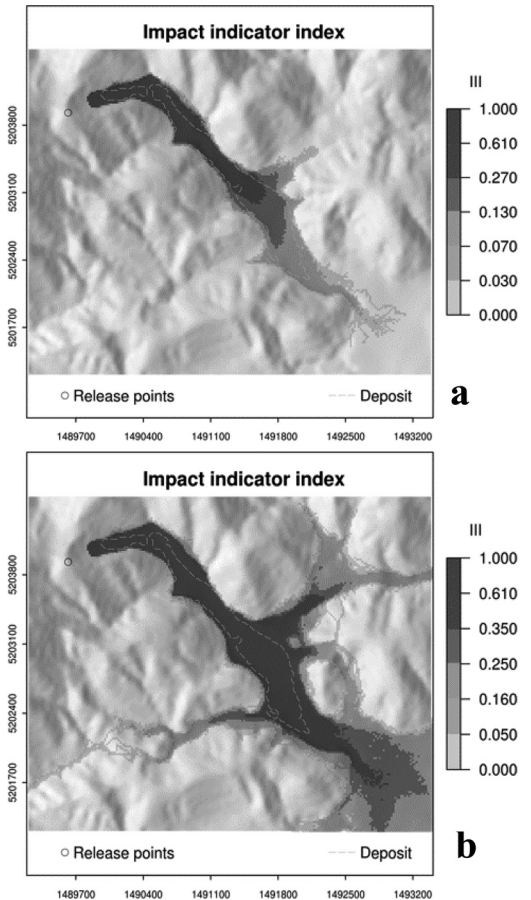


Figure 11. Comparison of resulting maps (Acheron) of r.randomwalk; a:  $AUC_{ROC} = 0.869$  b:  $AUC_{ROC} = 0.963$ .

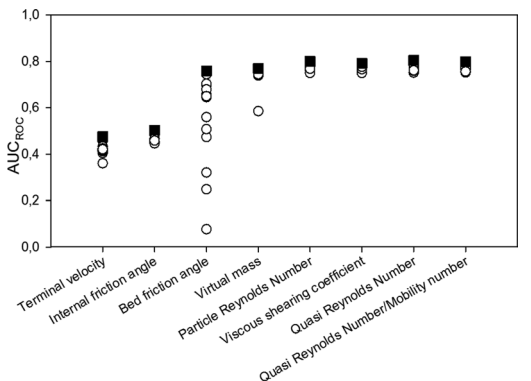


Figure 12. r.avaflow: Optimization procedure for the Acheron Rock Avalanche (markers: white = 1st cycle, black = maximum value).

After the first two steps the  $AUC_{ROC}$  values (0.503) indicate a random prediction. However, a significant increase occurs after the optimization of the bed friction angle (see Fig. 12). The  $AUC_{ROC}$  values peak at 0.804, reached after testing the Quasi Reynolds number. In fact the  $AUC_{ROC}$  values stay approximately constant during the last four optimization steps. Again the slight deviations here are likely to originate from the randomness in the parameter distribution.

The result shows that the bed friction angle seems to have by far the most influence on the quality of the result, followed by the internal friction angle and the particle Reynolds number. For the considered event and the chosen order of parameter optimization, variations of all other parameters lead to small changes of  $AUC_{ROC}$ . However, changing the order of the parameters might lead to different results and still needs to be investigated.

We note that (i) not all relevant input parameters of *r.avafow* are considered in this preliminary test of the optimization procedure and (ii) that the simulation tool is still in the development phase and therefore subject to ongoing improvement work.

## 5 DISCUSSION

In general, testing the proposed parameter optimization procedure has led to promising results. In contrast to the widely applied one-at-a-time approach, the suggested method accounts for parameter interference, avoiding the return to the starting values after each step (Saltelli et al. 2010).

We have shown that during the first optimization cycle the  $AUC_{ROC}$  values indicate a significant improvement after each step. However, during the second cycle the results do not improve notably. This might indicate that it is not always necessary to conduct two cycles if focusing on the  $AUC_{ROC}$  values. On the other hand, some value ranges feature a concretization during the second cycle.

A larger number of case studies is necessary to conclude on this issue as well as to confirm and to confine the ranges of the obtained guiding values. Further, the guiding values have to be applied to forward calculations of different events in order to assess their predictive power.

Considering the application of the procedure to a large number of case studies and various types of processes, an issue of particular concern is the large number of values to optimize. This requires a very high number of simulation runs—and therefore, consumes a lot of computational time to cover the multi-dimensional space of parameter values in appropriate detail. The 100 model runs performed for *r.randomwalk* and the 48 runs for *r.avafow* only serve for demonstrating the procedure.

To face this challenge we next intend to (i) test how many model runs are required for each random combination of parameter ranges to yield stable results, (ii) introduce a more efficient controlled approach of parameter variation, (iii) explore a computational cluster to decrease computational time, and (iv) test our procedure against other procedures such as AIMEC (Fischer 2013) in terms of time efficiency and results.

A subject of further investigation consists in identifying those parameters strongly influencing the simulation results, and therefore requiring particular attention. Even though the suggested procedure does not represent a sensitivity analysis in the strict sense, it still provides some information on the contribution of each parameter to the simulation result.

Our choice to focus on ranges of input parameter values instead of single values is supported by the finding that using ranges generally yields the higher  $AUC_{ROC}$  values. However, this issue requires further investigation as  $AUC_{ROC}$  values derived with ranges and with single values might not be fully comparable. Further, other indicators might be used in addition or alternatively to  $AUC_{ROC}$ .

## 6 CONCLUSIONS AND OUTLOOK

We have presented a stepwise procedure to optimize the input parameters for mass flow simulation approaches. The proposed method focuses on ranges of input parameter values instead of single values. The procedure was applied with the conceptual tool *r.randomwalk* and the advanced physically-based tool *r.avafow*, employing two rock avalanches as case studies. Optimization was based on  $AUC_{ROC}$  values derived from the comparison of simulation result to the observed deposition area.

Testing the proposed procedure yielded promising results. At the current development stage and with the specific settings chosen, *r.randomwalk* simulations for now seem to result in higher  $AUC_{ROC}$  values when reproducing the observed deposition area of the Acheron Rock Avalanche than the physically-based simulation tool *r.avafow*. However, this statement is still preliminary and might have to be revised along with the ongoing further development of *r.avafow*.

The present work is only seen as a first step towards obtaining guiding values—or ranges of values—of the input parameters for various types of mass flow processes. In this sense it represents a starting point for discussion rather than as the presentation of definitive results. The next steps will consist in (i) making the procedure more powerful and time-efficient, (ii) extending the number of events tested, (iii) evaluating the guiding parameter

ranges obtained by performing forward calculations of independent events, and (iv) applying (ii) and (iii) to other types of mass flow processes.

## ACKNOWLEDGEMENTS

The work was conducted as part of the international cooperation project “A GIS simulation model for avalanche and debris flows (avaflow)” supported by the Austrian Science Fund (FWF, project number I 1600-N30) and the German Research Foundation (DFG, project number PU 386/3-1).

## REFERENCES

- Baumann, V. 2011. Debris flow susceptibility mapping at a regional scale along the National Road N7, Argentina. Proceedings of the 14th Pan-American Conference on Soil Mechanics and Geotechnical Engineering.
- Fischer, J.-T. 2013. A novel approach to evaluate and compare computational snow avalanche simulation. *Natural Hazards & Earth System Sciences* 13: 1655–1667.
- Gamma, P. 2000. dfwalk—Ein Murgang-Simulationssprogramm zur Gefahrenzonierung. *Geographica Bernensia* G66.
- GRASS Development Team: Geographic Resources Analysis Support System (GRASS) Software, Version 7.0. Open Source Geospatial Foundation, available at: <http://grass.osgeo.org>, last access 27 July 2015.
- Jibson R.W., Harp, E.L., Schulz, W., Keefer, D.K. 2006. Large rock avalanches triggered by the M 7.9 670 Denali Fault, Alaska, earthquake of 3 November 2002. *Eng. Geol.* 83: 144–160.
- Jónasson, K., Sigurdsson, S.P., Arnalds, B. 1999. Estimation of avalanche Risk. *Íslands, Rit Veðurstofu*.
- Mergili, M., Fischer, J.-T., Fellin, W., Ostermann, A., Pudasaini, S.P. 2015a. r.avaflow: An advanced open source computational framework for the GIS-based simulation of two-phase mass flows and process chains. *EGU General Assembly*, Vienna, April 12–17, 2015. *Geophysical Research Abstracts* 17.
- Mergili, M., Krenn, J., Chu, H.-J. 2015b. r.randomwalk v1, a multi-functional conceptual tool for mass movement routing. *Geoscientific Model Development* 8: 4027–4043.
- Mergili, M., Schratz, K., Ostermann, A., Fellin, W. 2012: Physically-based modelling of granular flows with Open Source GIS. *Natural Hazards and Earth System Sciences* 12: 187–200.
- Perla, R., Cheng, T.T., McClung, D.M. 1980. A two-parameter model of snow-avalanche motion. *Journal of Glaciology* 26: 197–207.
- Pudasaini, S.P. 2012. A general two-phase debris flow model. *Journal of Geophysical Research: Earth Surface* 2003–2012, 117(F3).
- Pudasaini, S.P. 2014. Dynamics of Submarine Debris Flow and Tsunami. *Acta Mechanica*, Vol. 225(8), 2423–2434.
- Pudasaini, S.P., Michael Krautblatter. 2014. A two-phase mechanical model for rock-ice avalanches. *J. Geophys. Res. Earth Surf.* 119.
- Saltelli, A., Annoni, P. 2010. How to avoid a perfunctory sensitivity analysis. *Environmental Modelling & Software* 25: 1508–1517.
- Shugar, D.H., Clague, J.J. 2011. The sedimentology and geomorphology of rock avalanche deposits on glaciers. *Sedimentology* 58: 1762–1783.
- Smith, G.M., Davies, T.R., McSaveney, M.J., Bell, D.H. 2006. The Coseismicity and Morphology of the Acheron Rock Avalanche Deposit in the Red Hill Valley, New Zealand. *Landslides* 3: 62–72.
- Sosio, R., Crosta, G.B., Chen, J.H., Hungr, O. 2012. Modelling of rock avalanche propagation onto glaciers. *Quaternary Science Reviews* 47: 23–40.
- Vilajosana, I., Surñach, E., Khazaradze, G., Gauer, P. 2007. Snow avalanche energy estimation from seismic signal analysis. *Cold Regions Science and Technology* 50: 72–85.
- Wichmann, V., Becht, M. 2003. Modelling of geomorphic processes in an Alpine catchment. *GeoDynamics*: 151–167.
- Zimmermann, M., Mani, M., Gamma, P., Gsteiger, P., Heiniger, O., Hunziker, G. 1997. *Murganggefahr und Klimaänderung—ein GIS-basierter Ansatz*. vdf Hochschulverlag AG, ETH Zürich: 162.